Rev. Roum. Sci. Techn.– Électrotechn. et Énerg.
Vol. 61, *3*, pp. 244–249, Bucarest, 2016

DIRECT TORQUE CONTROL OF WIND TURBINE DRIVEN DOUBLY FED INDUCTION GENERATOR

SALAH TAMALOUZT[1], KASSA IDJDARENE[1], TOUFIK REKIOUA[1], RACHID ABDESSEMED[2]

Key words: Doubly fed induction generator (DFIG), Direct torque control (DTC), Random behavior wind speed, Maximum power point tracking (MPPT), Pitch angle control.

The aim of the present paper is to show the analysis of the direct torque control technique (DTC) performances applied to a doubly fed induction generator (DFIG) driven by a wind turbine (WT), taking into account the randomness of wind allowing the three modes operation (sub, super and synchronous) of the DFIG, with a particular focus on synchronous and the over-speed modes. The captured wind energy is optimized to extract the maximum power using the maximum power point tracking (MPPT) algorithm. Beyond the nominal turbine speed, we will be acting on the pitch angle control. The studied system control is tested and validated through numerical simulation. The obtained results show the effectiveness of the control strategy leading to best performances.

1. **INTRODUCTION**

Nowadays, a greater emphasis is given to renewable energies, particularly wind, which is one of the most-effective systems available to generate electricity [1]. In the case of grid connected wind energy, the DFIG remains widely used. The reasons for the popularity of DFIGs are the potential of delivering high yields in regard to energy production and allowing an independent control of active and reactive power generation [2] without using capacitors for reactive power control. Since the converter is only used to control the power in the rotor windings, which is a fraction of the output power from the DFIG. Thus, the power loss and the size of the power electronic converters for DFIGs are smaller than those of conventional full-size stator converters [3].

In the aim to develop a quiet, efficient, and economical grid connected wind energy conversion systems (WECSs), different control algorithms applied to DFIG have been proposed in the literature [4–23]. Conventional control scheme is usually based on two most control methods families, i.e., field-oriented control (FOC) [4–12], and direct control techniques namely the direct torque control or the direct power control (DPC) [13–23]. Linear vector control (LVC) methods have been widely applied to DFIG with operation in different quadrants in many research works [4–6]. Due to both the nonlinear nature of the inverter, of finite possible states, and the linear time-varying nature of the machine model, the nonlinear control techniques such as sliding mode vector control (SMC) [7], model reference adaptive control (MRAC) [8], fuzzy logic vector control [9], predictive control [10], artificial neural networks (ANN) [11] and combinations of some previous techniques [12], produce control laws with a rather high computational burden. Consequently, the complexity of the control system is increased. These computations commonly depend on the system states and also on several model parameters having the secondary effect of reducing the control robustness. Other control techniques, like SMC techniques produce high frequency discontinuous control actions. Some others necessitate neglecting the voltage drop across the stator leakage impedance; this assumption leads to a steady-state error in the system operation. On the other hand, DPC [13, 14] and DTC [15–23] are widely used as another alternative to the LVC. The DTC approach is employed taking advantage of the main features of this control concept, i.e., lower machine parameters dependency, simpler structure, does not require any coordinate transformation and specific modulations, high dynamic performances and minimal response time, achieving better steady state and transient torque control conditions than field oriented control (FOC) [13]. The torque control performances of DFIG are mainstream to reduce mechanical constraints and then to reduce the wear process on the gearbox which has been identified as one of the most critical system components [18].

Many research works have already been done in this context. Indeed, this strategy has been proposed to control the DFIG flux and torque only in the sub-synchronous mode or super-synchronous mode [15–17]. Other authors have been studied the sub-synchronous and the super-synchronous modes either separately [18], or together [19, 20] considering the synchronous mode as a simple point to permit the passage between the two modes. Due to the random behavior of the wind, the synchronous mode of the DFIG can take a considerable time interval, so the study of this mode becomes a necessity. In this case, there are only two authors [22, 23] interested to the three modes operating of the DFIG. In [22], the three modes were studied separately, where a DTC-SVM technique of the DFIM is presented. A nonlinear controller was introduced based on the input-output feedback linearization control method for a DFIG, using a two layer ANN. Consequently, the complexity of the system control is increased. The neural networks-based controllers present the drawback of not being systematic in the design stage nor providing a rigorous stability proof. However, only the authors of [23] have treated these three modes in a successive and continuous manner. But, the aim of their work is just for showing the behavior of the DFIG in each mode, by using a fixed wind speed in each operating mode of this generator. Instead of using one converter in the rotor circuit, two converters are used in each side of a DFIM, i.e., the rotor and the stator [18]. One converter controls the stator flux while the other controls the rotor flux. This method, known as the dual-DTC strategy, uses two switching tables for the stator and rotor converters. Although, interesting features and more degree of freedom

[1] Université de Bejaia, Faculté de Technologie, Laboratoire de Technologie Industriel et de l'Information, 06000, Algerie, E-mail: tamalouztsalah@yahoo.fr, idjdarene@yahoo.fr, to_reki@yahoo.fr
[2] Université de Batna, Faculté de Technologie, Laboratoire d'Electrotechnique de Batna, 05000, Algerie, E-mail: rachid.abdessemed@gmail.com.

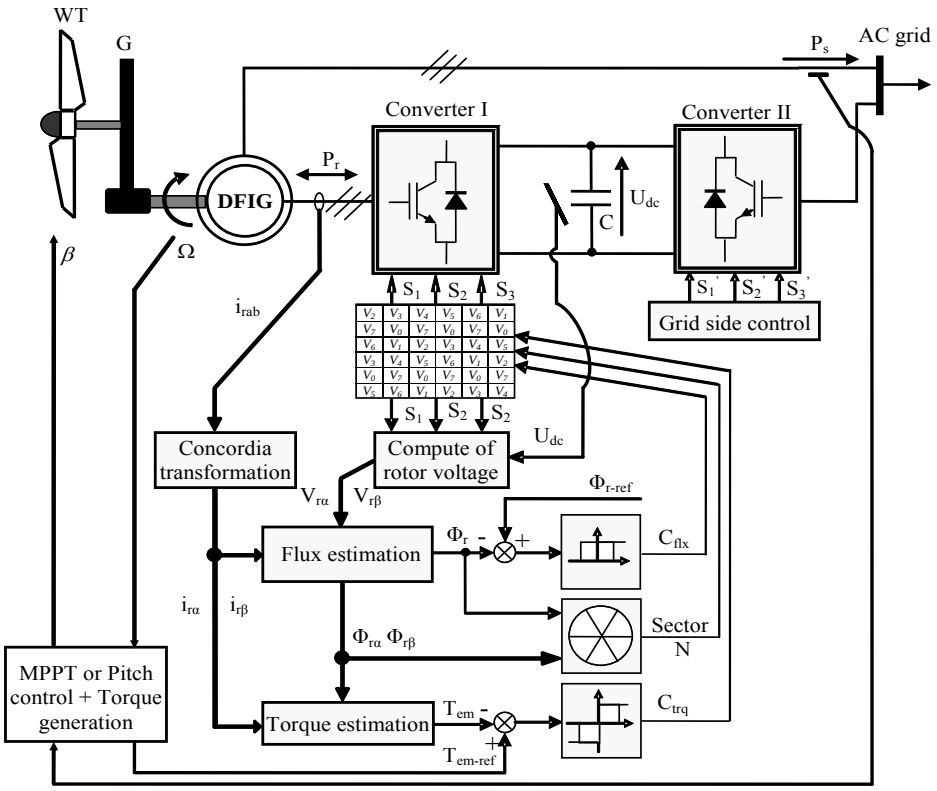

Fig. 1 – The studied system.

arise by using the dual-DTC approach, higher complexity and an increase in the cost of the system are inevitable.

The aim in the present paper is to analyze the performances of the DTC technique applied to a DFIG, taking into account the randomness of wind allowing the three operation modes (sub, super and synchronous), with a particular focus on synchronous and the over-speed modes. The quality and performances of this technique are examined in the case of the stochastic nature of wind in the most interesting operating zones of WT characteristic. The most important zone is where the captured wind energy is optimized to extract the maximum power using the MPPT algorithm. Beyond the nominal turbine speed, maintaining constant the reference speed is necessary. When the nominal power is reached, power extraction maximization amounts to regulate the power produced at its rate value, acting on the blades pitch angle. The effectiveness of the proposed strategy is validated by simulation tests under MATLAB/SIMULINK.

2. DESCRIPTION AND MODELING OF WT-DFIG SYSTEM

The turbine aerodynamic torque T_t is given by the following relation [23]:

$$T_t = \frac{1}{2} C_p \frac{\rho \pi R^2}{\Omega_t} v^3, \tag{1}$$

where, v, ρ and R are respectively the wind speed, the air density and the rotor radius. Besides, C_p and Ω_t are the power coefficients and the turbine rotor speed. The power coefficient for WT model is given as a function of tip-speed ratio and the blade pitch angle (β). To determine the power coefficient, we have used in this work, the following expression:

$$C_p(\lambda,\beta) = 0.5176\left[116\left(\frac{1}{\lambda_i}\right) - 0.4\beta - 5\right]\exp\left(-\frac{21}{\lambda_i}\right) \cdot 0.0068.\lambda_i, \tag{2}$$

$$\frac{1}{\lambda_i} = \frac{1}{\lambda + 0.08.\beta} - \frac{0.035}{1+\beta^3}. \tag{3}$$

The two-phase model of the DFIM expressed in the rotor frame is used. The classical electrical equations are written in this frame, as follows:

$$\begin{bmatrix} v_{sd} \\ v_{sq} \\ v_{rd} \\ v_{rq} \end{bmatrix} = \begin{bmatrix} R_s & -p\Omega L_s & 0 & -p\Omega M \\ p\Omega L_s & R_s & p\Omega M & 0 \\ 0 & 0 & R_r & 0 \\ 0 & 0 & 0 & R_r \end{bmatrix} \cdot \begin{bmatrix} i_{sd} \\ i_{sq} \\ i_{rd} \\ i_{rq} \end{bmatrix} + \begin{bmatrix} L_s & 0 & M & 0 \\ 0 & L_s & 0 & M \\ M & 0 & L_r & 0 \\ 0 & M & 0 & L_r \end{bmatrix} \cdot \begin{bmatrix} \frac{di_{sd}}{dt} \\ \frac{di_{sq}}{dt} \\ \frac{di_{rd}}{dt} \\ \frac{di_{rq}}{dt} \end{bmatrix}, \tag{4}$$

where R_s, R_r, l_s and l_r are the phase resistances and leakage inductances respectively. The M represents the magnetizing inductance, Ω is the mechanical speed and p, the pair pole number. Besides v_{sd}, v_{sq}, i_{sd} and i_{sq} are the d-q stator voltage and currents, respectively. While the v_{rd}, v_{rq}, i_{rd} and i_{rq} are the rotor voltage and currents, along the d-q axis, respectively.

3. **DIRECT TORQUE CONTROL**

The DTC is based on the regulation of the rotor flux magnitude and the value of the machine electromagnetic torque. The magnitude of the rotor flux is estimated from its components along the α and β axes [23]:

$$\begin{cases} \Phi_{r\alpha}(t) = \int_0^t (v_{r\alpha} - R_r i_{r\alpha})\,dt, \\ \Phi_{r\beta}(t) = \int_0^t (v_{r\beta} - R_r i_{r\beta})\,dt, \end{cases} \quad (5)$$

$$\Phi_r = \sqrt{\Phi_{r\alpha}{}^2 + \Phi_{r\beta}{}^2}\,. \quad (6)$$

The electromagnetic torque can be estimated starting from the estimated value of the flux ($\Phi_{r\alpha}$, $\Phi_{r\beta}$) and the calculated values of the current ($i_{r\alpha}$, $i_{r\beta}$) [23]:

$$T_{em} = p(\Phi_{r\alpha} i_{r\beta} - \Phi_{r\beta} i_{r\alpha}). \quad (7)$$

4. **PITCH ANGLE CONTROL**

WT controller objectives depend on the operating zone (Fig. 2)**.** In region I it must extract a maximum power from the wind. Region II covers a wind speed range between v_{n0} and v_{rated} and is referred as a transition between maximum power curve of region I and maximum power ($P_{s\text{-}max}$) in region III. This one covers a wind speed range between v_{rated} and $v_{cut\text{-}out}$ and is referred as the above-rated wind speed region. As the mechanical power generated by the rotor is limited, the main task of the controller in this region is to keep output at its rated power. This is generally achieved by holding the generator torque constant and varying the blade pitch angle.

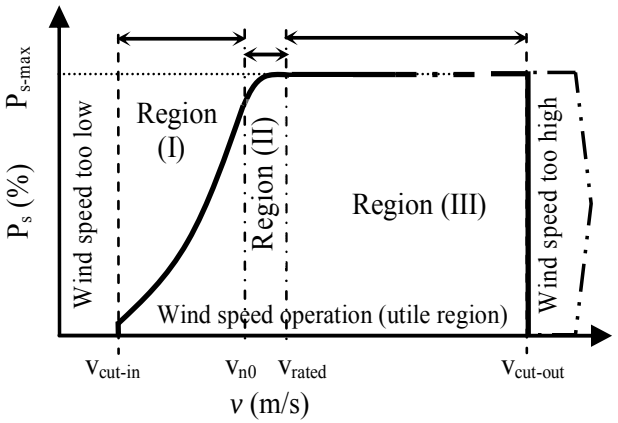

Fig. 2 – Operation regions of wind turbine.

This works deals especially with regions I and III for WT control. Two control inputs are available: the generator torque and the blade pitch angle, the latter is generated based on the power error to maintain the power to its maximum value, while the torque controller maintains the rotor speed within acceptable limits, as presented in Fig. 3. The linear proportional integral (PI) controller is used for power regulation, stator (P_s) and rated power (P_n) generation, to control the blade pitch angle, given by the following relation:

$$\dot{\beta} = \frac{d\beta}{dt} = K_p\,(P_n - P_s) + K_i \int (P_n - P_s)\,dt\,, \quad (8)$$

where $P_n - P_s$ is the tracking error.

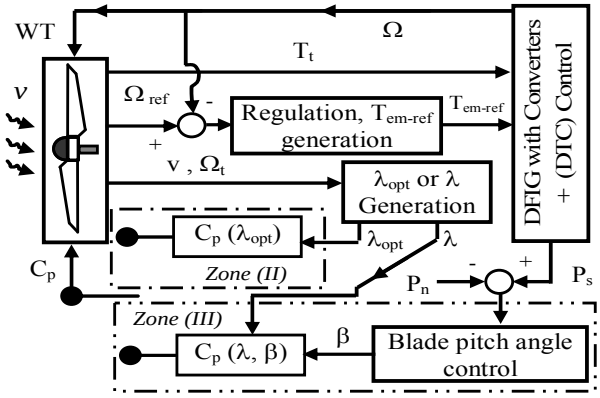

Fig. 3 – Wind turbine control.

5. **SIMULATION RESULTS**

The performances and the robustness of the proposed control under a random behavior of the wind speed in each mode (sub-synchronous, super-synchronous and synchronous modes) are shown in this section, for successive and continuous manner of the DFIG operation. The system parameters are given in [24].

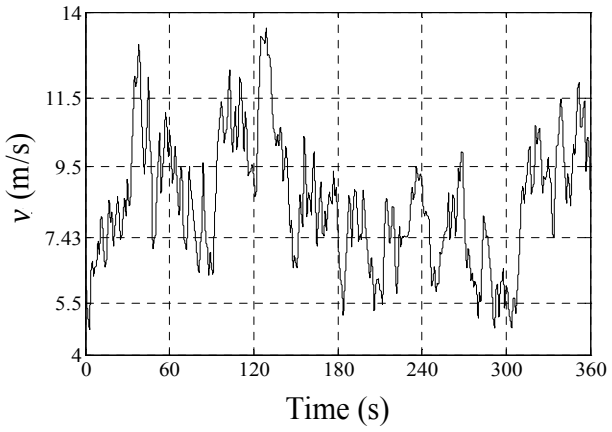

Fig. 4 – Waveform of the wind speed.

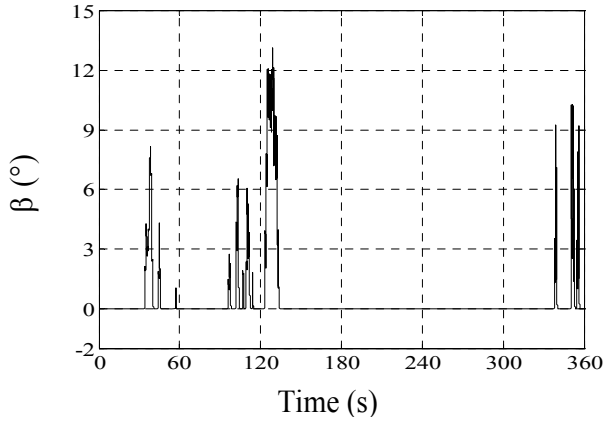

Fig. 5 – Waveform of the blade pitch angle.

The wind speed profile is given in Fig. 4. The control objective of this section is to show the performance in both interest operation regions (I and III) of the WT characteristic. In the region III, one can see that the stator power is limited at its maximum value by the pitch angle control, as shows Fig. 5. This is approved by the waveforms illustrated in Figs. 5 and 6 of the blade pitch angle, tip speed ratio and the power coefficient. We can observe that, when the power attained its maximum value ($P_{s\text{-}max}$), the pitch angle control is activated, and then the blade pitch angle varies introducing the variation of the tip speed ratio and the power coefficient.

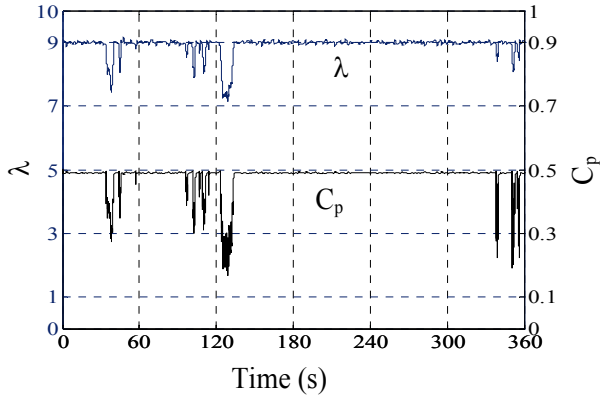

Fig. 6 – Waveform of the tip-speed ratio and power coefficient.

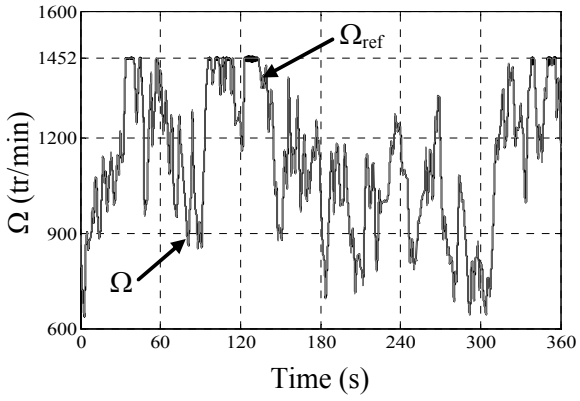

Fig. 7 – Waveform of the mechanical speed and its reference.

The mechanical speed is kept constant, at its limit value, as plotted in Fig. 7. Then, as expected, the electromagnetic torque is maintained constant, as shown in Fig. 8. However, in region I the power is maximized by the MPPT algorithm. In this case, as expected, the blade pitch angle, tip speed ratio and the power coefficient are maintained at constant values ($\beta = 0$, $\lambda = \lambda_{opt} = 9$, $C_p = C_{p\text{-}max} = 0.49$).

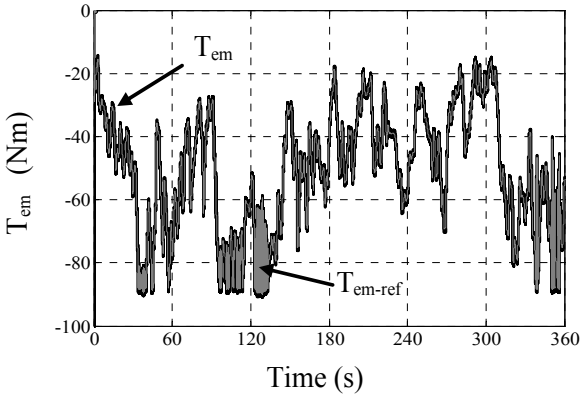

Fig. 8 – Waveform of the electromagnetic torque and its reference.

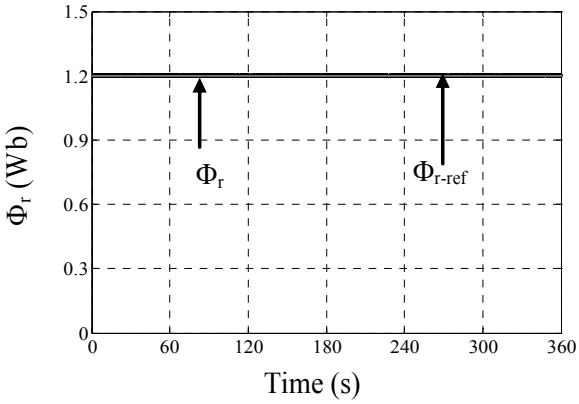

Fig. 9 – Waveform of the magnitude of rotor flux and its reference.

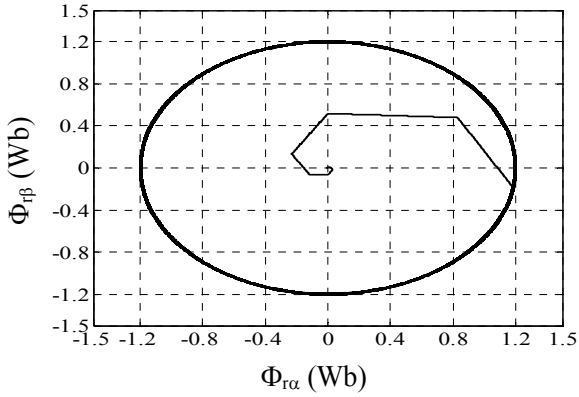

Fig. 10 – Waveform of the rotor flux.

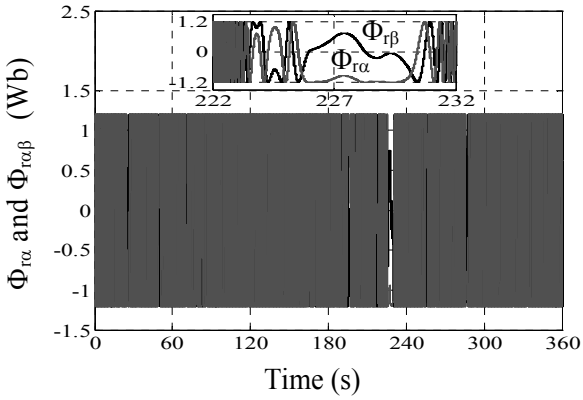

Fig. 11 – Waveform of the flux $\Phi_{r\alpha}$ and $\Phi_{r\beta}$.

The waveforms of the mechanical speed, electromagnetic torque and the magnitude of the rotor flux, with their references are illustrated respectively in Figs. 7, 8 and 9. They show reference tracking reflecting the robustness of the proposed control under random behavior of wind speed. Fig. 10 shows the rotor flux waveform, it is circular and kept constant at 1.2 Wb. This form of rotor flux leads to a sinusoidal behavior of the fluxes $\Phi_{r\alpha}$ and $\Phi_{r\beta}$ (Fig. 11) in the sub-synchronous and super-synchronous modes. In the synchronized asynchronous mode the fluxes ($\Phi_{r\alpha}$ and $\Phi_{r\beta}$) have continuous behavior and take their values in such a way to maintain constant the flux magnitude.

It is then clear from the obtained results that random change in wind speed imposes a successive and a continuous operation to the DFIG in the three modes. The transition

between the sub-synchronous ($s > 0$) to the super-synchronous mode ($s < 0$) or vice-versa is realized through the synchronous mode in an obvious manner, as shown by the slip (Fig. 12) and the rotor active power (Fig. 13) waveforms. This makes the synchronous mode very important and not neglected in the operation of the DFIG. This last mode illustrated by a direct form of the phase rotor current (Fig. 14) and the slip $s = 0$ as presented in Fig. 12. The continuous behavior of the rotor current implies reactive power in the rotor. The random evolution of the rotor current magnitude is related to the electromagnetic torque variations and their pulsation is depending on the slip variations.

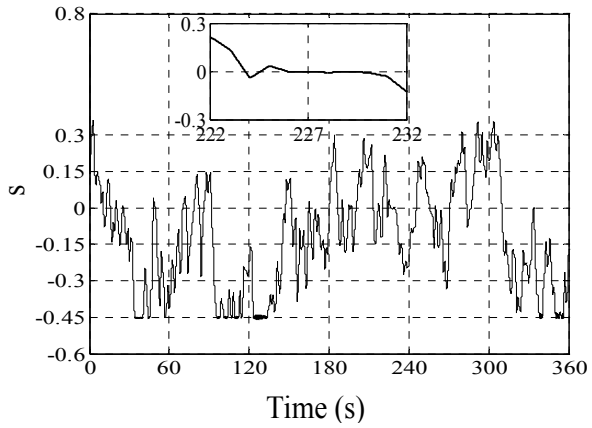

Fig. 12 – Waveform of the DFIG slips.

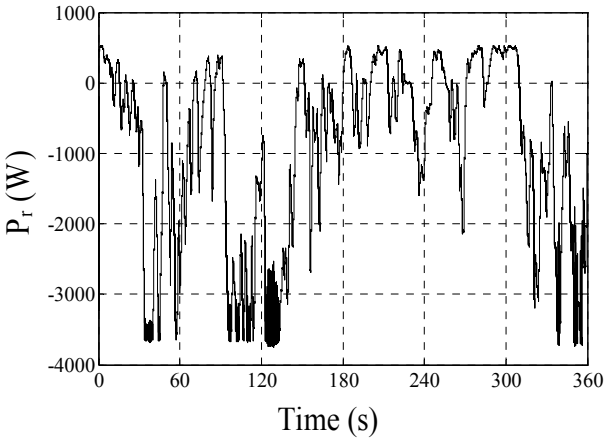

Fig. 13 – Waveform of the rotor active power.

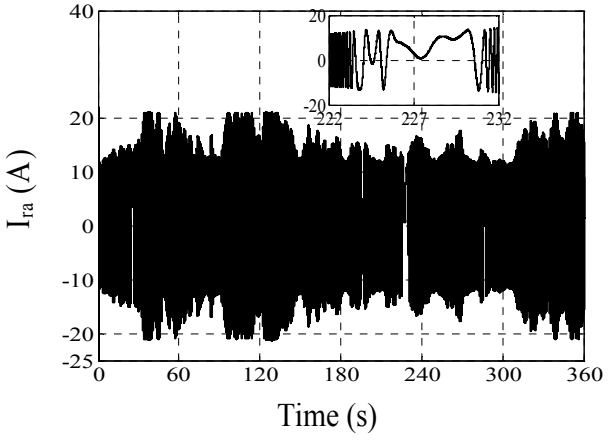

Fig. 14 – Waveform of the rotor current.

The operation as a generator is illustrated by the negative sign of the stator active power ($P_s < 0$), with a variable amplitude, which depends on the wind speed evolution, as presented in Fig. 15 where it can be seen that the operation with constant power is clear within the over-speed zone.

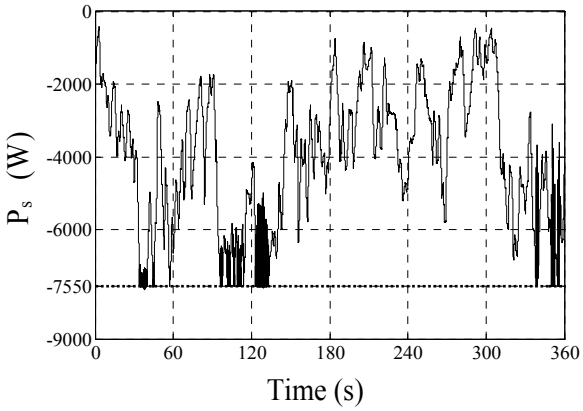

Fig. 15 – Waveform of the stator active power.

11. **CONCLUSIONS**

The aim of this work is to analyze the DTC strategy performances applied to control the DFIG rotor flux and electromagnetic torque, taking into account the randomness of wind allowing the three modes (sub, super and synchronous) operation, with a particular focus on synchronous and the over-speed modes, where, the references tracking and the robustness of the proposed control is investigated. We were interested to the operation in the regions I and III of the WT characteristic. In the region III the aim is to show that the power is limited at its maximum value by the pitch angle control but in the region I the aim is to maximize the extracted power. The obtained results show clearly satisfactory performances of the DFIG control in the three operation modes. The interest of using DFIG in the synchronized asynchronous mode is due to its ability to operate as synchronous generator unlike the induction generator. Then, we have a continuous behavior of the rotor voltage and current, which induces a rotor zero reactive power, which confirm the effectiveness proposed control.

Received on March 13, 2015

REFERENCES

1. B. Sawetsakulanond, V. Kinnares, *Design, analysis, and construction of a small scale self-excited induction generator for wind energy application*, Energy Journal, **35**, pp. 4975–4985 (2010).
2. A. Tapia, G. Tapia, J.X. Ostolaza, J.R. Saenz, *Modeling and control of a wind turbine driven doubly fed induction generator*, IEEE Trans. Energy Convers., **18**, *2*, pp. 194–204 (2003).
3. K.C. Wong, S.L. Ho, K.W.E. Cheng, *Direct torque control of a doubly-fed induction generator with space vector modulation*, Elec. Pow. Comp. and Syst., **36**, *12*, pp. 1337–1350 (2008).
4. E.G. Shehata, *Active and reactive power control of doubly fed induction generators for wind energy generation under unbalanced grid voltage conditions,* Elec. Pow. Comp. and Syst., **41**, *6*, pp. 619–640 (2013).
5. M. Rahimi, M. Parniani, *Dynamic behavior analysis of doubly-fed induction generator wind turbines, the influence of rotor and speed controller parameters*, Int. J. of Elec. Pow. and Energy Syst., **32**, *5*, pp. 464–477 (2010).

6. K. Kerrouche, A. Mezouar, K. Belgacem, *Decoupled control of doubly fed induction generator by vector control for wind energy conversion system*, Energy Procedia, **42**, pp. 239–248 (2013).
7. M. Adjoudj, M. Abid, A. Aissaoui, Y. Ramdani, H. Bounoua, *Sliding mode control of a doubly fed induction generator for wind turbines,* Rev. Roum. Sci. Techn. – Electrotechn. et Energ., **56**, *1*, pp. 15–24 (2011).
8. S. Abdeddaim, A. Betka, S. Drid, M. Becherif, *Implementation of MRAC controller of a DFIG based variable speed grid connected wind turbine*, Energ. Conv. and Manag., **79**, pp. 281–288 (2014).
9. M. Pichan, H. Rastegar, M. Monfared, *Two fuzzy-based direct power control strategies for doubly-fed induction generators in wind energy conversion systems*. Energ., **51**, pp. 154–162 (2013).
10. K. Ouari, T. Rekioua, M. Ouhrouche, *Real time simulation of nonlinear generalized predictive control for wind energy conversion system with nonlinear observer*, ISA Trans., **53**, *1*, pp. 76–84 (2014).
11. O. Soares, H. Gonçalves, A. Martins, A. Carvalho, *Nonlinear control of the doubly-fed induction generator in wind power systems,* Renew. Energ., **58**, *8*, pp. 1662–1670 (2010).
12. A. Abdelfetteh, M. Abid, *Hybrid fuzzy sliding mode control of a doubly fed induction generator in wind turbines,* Rev. Roum. Sci. Techn. – Electrotechn. et Energ., **57**, *4*, pp. 15–24 (2012).
13. G. Abad, M.A. Rodriguez, G. Wanski, L. Poza, *Direct power control of doubly fed induction-generator based wind turbines under unbalanced grid voltage*, IEEE Trans. on Pow. Electro., **25**, *2*, pp. 586–588 (2010).
14. L. Shang, J. Hu, *Sliding-mode-based direct power control of grid-connected wind-turbine-driven doubly fed induction generators under unbalanced grid voltage conditions*, IEEE Trans. On Energ. Conver., **27**, 2, pp. 362–373 (2012).
15. A.M. El-Sawy, A.A. Hassan, O.M. Kamel, *Direct torque control using direct matrix converter for doubly fed induction generator driven by variable speed wind turbine*, Minia Journal of Engineering and Technology (MJET), **32,** *1*, pp. 109–121 (2013).
16. Y. Sreenivasa Rao, A. Jaya Laxmi, *Direct torque control of doubly fed induction generator based wind turbine under voltage dips,* International Journal of Advances in Engineering & Technology (IJAET), **3**, *2*, pp. 711–720 (2012).
17. G. Naveen, P.K.S. Sarvesh, B. Rama Krishna, *DTC control strategy for doubly fed induction machine*, International Journal of Engineering and Advanced Technology (IJEAT), **3**, *1*, pp. 92–95 (2013).
18. F. Bonnet, P.E. Vidal, M. Pietrzak-David, *Dual direct torque control of doubly fed induction machine*, IEEE Trans. on Ind. Electro., **54**, *5*, pp. 2482–2490 (2007).
19. J. Arbi, M.J. Ben Ghorbal, I. Slama-Belkhodja, L. Charaabi, *Direct virtual torque control for doubly fed induction generator grid connection*, IEEE Trans. on Ind. Electron., **56**, *10*, pp. 4163–4173 (2009).
20. J. Ben Alaya, A. Khedher, M. F. Mimouni, *Speed-sensorless DFIG wind drive based on DTC using sliding mode rotor flux observer*, Int. J. of Renew. Energ. Res., **2**, *4*, pp. 735–745 (2012).
21. J. Hua, X. Yuan, *VSC-based direct torque and reactive power control of doubly fed induction generator*, Renewable Energy, **40**, *1*, pp. 13–23 (2012).
22. A.F. Payam, M.N. Hashemnia, J. Faiz, *Robust DTC control of doubly-fed induction machines based on input-output feedback linearization using recurrent neural networks*, Journal of Power Electronics (JPE), **11**, *5*, pp. 719–725 (2011).
23. S. Tamalouzt, T. Rekioua, R. Abdessamed, K. Idjdarene, *Direct torque control of grid connected doubly fed induction generator for the wind energy conversion*, Proc. of International Renewable Energy Congress IREC'2012, Sousse, Tunisia, December 19–22, 2012, pp. 1–6.
24. R.S. Pena, R.J. Cardenas, G.M. Asher, J.C. Clare, *Vector controlled induction machines for stand-alone wind energy applications*, Proc. of IEEE Ind. Appl. Conf., Rome, Italy, October 08–12, 2000, pp. 1409–1415.